Journal of Molecular Catalysis A: Chemical 309 (2009) 117–123

Contents lists available at ScienceDirect

Journal of Molecular Catalysis A: Chemical

journal homepage: www.elsevier.com/locate/molcata

Oxidation of activated methylene groups to ketones catalyzed by new iron phosphinooxazoline complexes and by iron(II) triflate

Matthew Lenze, Eike B. Bauer*

University of Missouri - St. Louis, Department of Chemistry and Biochemistry, One University Boulevard, St. Louis, MO 63121, USA

ARTICLE INFO

Article history:
Received 5 March 2009
Received in revised form 27 April 2009
Accepted 6 May 2009
Available online 15 May 2009

Keywords:
Iron
Catalysis
Oxidations
Phosphinooxazolines
Hydroperoxides

ABSTRACT

The study describes the first catalytic application of iron phosphinooxazoline complexes and $Fe(OTf)_2$ in oxidation reactions. New iron phosphinooxazoline (PHOX) complexes of the general formulation $[Fe(PHOX)_2]^{2+}[OTf]_2$ (**3**, $OTf = CF_3SO_3^-$) were synthesized in virtually quantitative yield from anhydrous $Fe(OTf)_2$ and the corresponding PHOX ligands. The new complexes **3** as well as previously synthesized iron PHOX complexes of the general formula $[Fe(Cp)(CO)(PHOX)]^+[I]^-$ (**2**) were employed as catalysts in the oxidation of benzylic CH_2 groups to the corresponding ketones. Whereas **3** showed catalytic activity at room temperature (about two equivalents *t*-BuOOH as the oxidant, 2 mol% catalyst, pyridine solvent, 12 h, 38–93% isolated yields), complexes of **2** were only active at elevated temperatures. The product profile is in accordance with a mechanism previously described as "oxygenated Fenton chemistry", which is further corroborated by UV–vis investigations. They showed that an iron alkylperoxo species [Fe–OO*t*Bu] might be involved in the catalytic cycle. The reaction follows a pseudo zero order rate law in substrate.

1. Introduction

Iron complexes have recently attracted considerable interest as catalysts in a variety of homogeneous organic transformations [1]. In general, iron is not the first choice when it comes to the development of novel catalyst systems, but it has a number of advantages over other transition metals (such as Pt, Pd, Rh, Ru or Au) typically utilized as catalysts in organic chemistry. It is cheap, abundant, non-toxic and environmentally friendly. Accordingly, an increasing number of publications describe the investigation of iron-based catalyst systems in transformations such as carbon–carbon [2a] and carbon–heteroatom bond forming reactions [2b], oxidations [2c,d], reductions [2e] and polymerizations [2f,g] and other reactions [2h]. Yields and selectivities are often comparable with other transition metal based catalyst systems, and therefore iron complexes have also been applied in natural product syntheses [3].

The majority of iron complexes to be employed in catalysis are generated *in situ*. Such systems are not necessarily more efficient than defined, preformed metal complexes. However, for mechanistic investigations as well as for studies regarding the relationship of ligand architecture and the activity of their respective iron complexes, the deployment of well-defined complexes could be advantageous.

We have recently synthesized and structurally characterized the first phosphinooxazoline chelate complexes of iron (**2**, Fig. 1) [4]. Phosphinooxazolines (PHOX, **1**) are a versatile bidentate ligand class [5], and were successfully employed in a variety of transition metal catalyzed asymmetric reactions [6]. However, to the best of our knowledge, iron PHOX chelate complexes have not yet been applied as catalysts thus far. Braunstein reported cyclopropanation and Diels–Alder reactions to be catalyzed by heterobimetallic iron copper complexes with bridging phosphinooxazoline ligands, in which only the phosphorus center is coordinated to the iron [7].

We were especially interested in the catalytic oxidation of alkanes. Alkanes tend to be rather unreactive; selective oxidation rapidly increases their structural complexity, and allows for further transformations. Accordingly, we first investigated the iron complex **2c** as catalyst for the oxidation of benzylic methylene groups with peroxides and observed activity (*vide infra*), but high reaction temperatures were required. We were thus interested to determine whether iron PHOX complexes with differing architectures would be more effective and could be employed at lower temperatures in the title reaction.

The objective of this study was to investigate alternatives to the coordinatively saturated iron PHOX complexes **2** (Fig. 1). For potential catalytic applications, complexes with the general formula $[Fe(\mathbf{1})_2]^{2+}[X^-]_2$ seemed to hold the greatest promise. In the case of weakly coordinating counterions X^-, such complexes feature two open coordination sites, a key requirement for catalytic activity. We synthesized such complexes and tested them in homogeneous catalytic oxidations of activated methylene groups utilizing peroxides

* Corresponding author. Tel.: +1 314 516 5340; fax: +1 314 516 5342.
E-mail address: bauere@umsl.edu (E.B. Bauer).

1381-1169/$ – see front matter © 2009 Elsevier B.V. All rights reserved.
doi:10.1016/j.molcata.2009.05.002

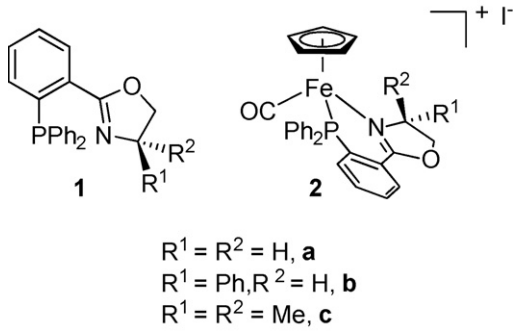

Fig. 1. Phosphinooxazoline (PHOX) ligands **1** and iron complexes **2** thereof.

as the oxidants. We also performed further experiments to better understand the mechanism of the iron catalyzed oxidations under investigation.

2. Experimental

2.1. General

Chemicals were treated as follows: acetonitrile was distilled from CaH_2. Other solvents, $CHCl_3$, pyridine, CH_2Cl_2, hexanes, the substrates for the catalytic experiments (Aldrich), and *t*-BuOOH (5.5 M in decane, Fluka) were used as received. Thoroughly dried $Fe(OTf)_2$ ($OTf = CF_3SO_3^-$) [8], iron complex **2c** [4] and the PHOX ligands **1a** and **b** [4] were synthesized according to the literature. Metal complex syntheses were carried out under argon employing standard Schlenk techniques. Workup as well as the catalytic experiments was performed under aerobic conditions.

The NMR spectra were obtained at room temperature on either a Bruker Avance 300 MHz or a Varian Unity Plus 300 MHz instrument and referenced to a residual solvent signal. GC/MS spectra were recorded on a Hewlett Packard GC/MS system model 5988A. Exact masses were acquired on a JEOL MStation [JMS-700] mass spectrometer. IR spectra were recorded on a Thermo Nicolet 360 FT-IR spectrometer. Elemental analyses were performed by Atlantic Microlab Inc., Norcross, GA, USA. Magnetic moments were determined by the Evans method [9].

$[Fe(\mathbf{1a})_2]^{2+}[OTf]_2$ ($[\mathbf{3a}]^{2+}$): To a Schlenk flask containing CH_3CN (2 mL) and $Fe(OTf)_2$ (0.053 g, 0.150 mmol), phosphinooxazoline **1a** (0.100 g, 0.301 mmol) was added and the solids dissolved. The resulting deep red solution was allowed to stir at room temperature for 10 min. The solvent was removed under high vacuum, yielding a red-orange solid. Anal. calcd for $C_{44}H_{36}F_6FeN_2O_8S_2P_2$: C, 51.98; H, 3.57. Found: C, 52.08; H, 3.83.

NMR (δ, CD_3CN) ^1H (full width at half maximum ca. 27Hz) 8.12 (dd, J_{HH} = 27 Hz, J_{HH} = 7 Hz, 2H, Ph), 8.04–7.07 (m, 23H, Ph), 6.96 (d, J_{HH} = 7.5 Hz, 2H, Ph), 6.68 (s, 1H), 4.76 (s, 2H, 2C*H*′H), 4.34 (s, 1H, C*H*′H), 3.82 (s, 1H, 2C*H*′H), 3.66 (s, 1H, C*H*′H), 3.19 (s, 2H, 2C*H*′H), 3.06 (s, 1H, C*H*′H); $^{13}C\{^1H\}$ (partial) 170.8 (s, *C*=N), 169.9 (s, *C*=N), 69.1 (s, *C*H_2), 68.4 (s, *C*H_2), 59.7 (s, *C*H_2), 55.2 (s, *C*H_2).

HRMS calcd for $C_{43}H_{36}F_3FeN_2O_5SP_2$ 867.1120; found 867.1105 (corresponds to $[Fe(\mathbf{1a})_2(OTf)]^+$). MS (FAB,3-NBA, *m*/*z*) [10]: 867 ($[Fe(\mathbf{1a})_2(OTf)]^+$, 35%), 536 ($[Fe(\mathbf{1a})(OTf)]^+$, 60%), 332 ($[\mathbf{1a}]^+$, 100%). IR ($cm^{-1}$, neat solid) $\nu_{C=N}$ 1627 (w), 1614 (w), ν_{SO} 1259 (s), ν_{CF} 1028 (s). Magnetic susceptibility (0.0108 M, CD_3CN), μ_{eff} = 2.26 BM.

$[Fe(\mathbf{1b})_2]^{2+}[OTf]_2$ ($[\mathbf{3b}]^{2+}$): To a Schlenk flask containing CH_3CN (2 mL) and $Fe(OTf)_2$ (0.043 g, 0.123 mmol), phosphinooxazoline **1b** (0.100 g, 0.246 mmol) was added and the solids dissolved. The resulting deep red solution immediately transitioned into dark brown. The solvent was removed under high vacuum, yielding a red-brownish solid. Anal. calcd for $C_{56}H_{44}F_6FeN_2O_8S_2P_2$: C, 57.54; H, 3.79. Found: C, 54.63; H, 3.93.

HRMS calcd for $C_{55}H_{44}F_3FeN_2O_6SP_2$ 1035.1679; found 1035.1670 (corresponds to $[Fe(\mathbf{1b})_2(O)(OTf)]^+$). MS (FAB,3-NBA, *m*/*z*)[10]: 1051 ($[Fe(\mathbf{1b})_2(O)_2(OTf)]^+$, 10%), 1035 ($[Fe(\mathbf{1b})_2(O)(OTf)]^+$, 5%), 628 ($[Fe(\mathbf{1b})(O)(OTf)]^+$, 30%), 612 ($[Fe(\mathbf{1b})(OTf)]^+$, 25%), 408 ($[\mathbf{1b}]^+$, 100%). IR ($cm^{-1}$, neat solid) $\nu_{C=N}$ 1604 (w), ν_{S-O} 1260 (s), ν_{C-F} 1028 (s). Magnetic susceptibility (0.0109 M, CD_3CN), μ_{eff} = 3.63 BM.

$[Fe(\mathbf{1a})(H_2O)_n]^{2+}[OTf]_2$: To a Schlenk flask containing 2.0 mL of CH_3CN and $Fe(OTf)_2$ (0.106 g, 0.3 mmol), phosphinooxazoline **1a** (0.100 g, 0.3 mmol) was added and the solids dissolved. The resulting deep red solution was stirred at room temperature for 5 min. The solvent was then removed under vacuum.

MS (FAB,3-NBA, *m*/*z*)[10]: 867 ($[Fe(\mathbf{1a})_2(OTf)]^+$, 35%), 536 ($[Fe(\mathbf{1a})(OTf)]^+$, 100%), 332 ($[\mathbf{1a}]^+$, 80%). IR ($cm^{-1}$, neat solid) ν_{OH} 3435 (br), $\nu_{C=N}$ 1657 (w), 1627 (w), ν_{SO} 1223 (s), ν_{CF} 1026 (m, s).

2.1.1. Magnetic moment determination

0.0108 M solutions of the metal complexes in CD_3CN were placed in a NMR tube, and as an internal standard, a capillary containing pure CD_3CN and TMS (1 mol%) was introduced into the tube. Proton NMR spectra were recorded, and the $\Delta\nu$ value for the CD_2HCN resonances determined (see Supporting Material). The magnetic moments were calculated according to the literature [9b].

2.1.2. General procedure for the catalytic experiments

The substrate fluorene (0.100 g, 0.602 mmol) was dissolved in pyridine (2.0 mL) and the catalyst $[\mathbf{3a}]^{2+}$ (0.012 g, 0.012 mmol) was added. The oxidant *t*-BuOOH (1.07 mmol, 0.195 mL of a 5.5 M solution in decane) was added and the red solution stirred at room temperature for 12 h. The product was isolated as a yellow powder (0.099 g, 0.55 mmol, 91%) by column chromatography (basic alumina, eluent $CHCl_3$/hexanes, 2:3).

NMR (δ, $CDCl_3$) ^1H 7.72–7.66 (m, 2H, aromatic), 7.61–7.49 (m, 4H, aromatic), 7.36–7.29 (m, 2H, aromatic); $^{13}C\{^1H\}$ 194.1 (s, C=O), 144.7 (s, aromatic), 135.0 (s, aromatic), 134.4 (s, aromatic), 129.4 (s, aromatic), 124.6 (s, aromatic), 120.6 (s, aromatic). IR (cm^{-1}, neat solid) $\nu_{C=O}$ 1710 (s).

2.1.3. UV–vis experiment in Fig. 4

To the metal complex $[\mathbf{3a}]^{2+}$ (0.002 g, 0.00196 mmol) pyridine (0.25 mL) was added, followed by *t*-BuOOH (0.25 μL of a 5.5 M solution in decane, 0.138 mmol). CH_2Cl_2 (1 mL) was immediately added and a UV–vis spectrum recorded. For comparison, an UV–vis spectrum under identical conditions without the *t*-BuOOH was recorded.

2.1.4. Reaction kinetics monitored by GC (Figs. 5 and 6)

The substrate fluorene (0.05 g, 0.30 mmol) was dissolved in pyridine (2.0 mL) and the catalyst $[\mathbf{3a}]^{2+}$ (0.0061 g, 0.006 mmol) was added. The oxidant *t*-BuOOH (0.53 mmol, 0.097 mL of a 5.5 M solution in decane) was added, and the solution stirred at room temperature. For analysis, aliquots were taken from the reaction mixture, filtered through a short pad of alumina (which was washed with 2 mL CH_2Cl_2), and injected into the GC instrument. The substrate decay over time was determined by the ratio of its signal intensity to the signal intensity of decane, which was the solvent for the *t*-BuOOH and served as internal standard.

3. Results and discussion

3.1. Catalyst syntheses

The iron PHOX complexes with the general formula $[Fe(\mathbf{1})_2]^{2+}[X]^-_2$ were obtained by reaction of the PHOX ligands with simple anhydrous iron salts FeX_2. Accordingly, when

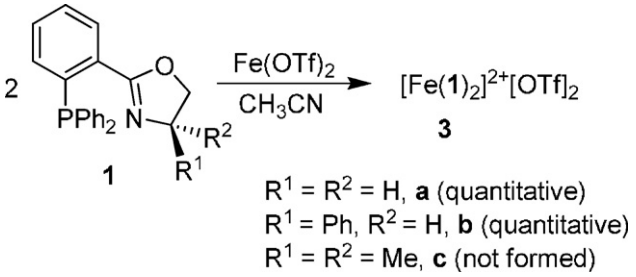

Scheme 1. Synthesis of iron PHOX complexes **3a** and **b**.

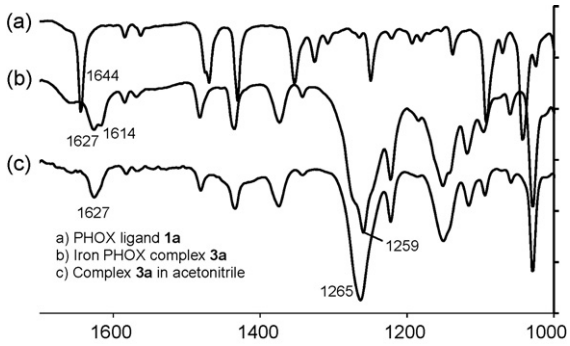

Fig. 2. IR spectra of PHOX ligand **1a** and its iron complex **3a**.

two equivalents of the ligands **1a**, **b** and **c** were combined with anhydrous $Fe(OTf)_2$ ($OTf = CF_3SO_3^-$) [8] in acetonitrile at room temperature for 10 min, the iron complexes $[Fe(\mathbf{1a})_2]^{2+}[OTf]_2$ ($[\mathbf{3a}]^{2+}$) and $[Fe(\mathbf{1b})_2]^{2+}[OTf]_2$ ($[\mathbf{3b}]^{2+}$) formed in virtually quantitative yield (Scheme 1). The complexes were isolated as red-orange and red-brown powders which will subsequently be referred to without charges and counterions. The complex **3b** did not give a correct elemental analysis and, somewhat surprisingly, no detectable coordination of ligand **1c** to the iron center was observed. No coordination of any of the ligands was observed, when $Fe(OAc)_2$ was employed as iron source; employment of anhydrous $FeCl_2$ gave the corresponding complex $Fe(\mathbf{1a})_2Cl_2$ and it showed somewhat less catalytic activity in the oxidation of diphenylmethane and fluorene (Table 1, entries 16 and 17) than **3a** [11].

For comparison, we also attempted the synthesis of the "mono-PHOX" iron complex $[Fe(\mathbf{1a})]^{2+}[OTf]_2$, containing only one PHOX ligand in the coordination sphere of the iron (Eq. (1)). As revealed by IR, the ligand coordinates to the iron, but also a strong OH peak around 3300 cm^{-1} was observed (which was absent in **3a** and **b**). We assume that when a deficiency of the PHOX ligand is employed, the open coordination site picks up water from the atmosphere (the complex liquefies when exposed to air for prolonged periods). In turn, the MS also exhibited a peak for $[Fe(\mathbf{1a})_2(OTf)]^+$ with two PHOX ligands on iron, corroborating the fact that the reaction in Eq. (1) gives multiple products:

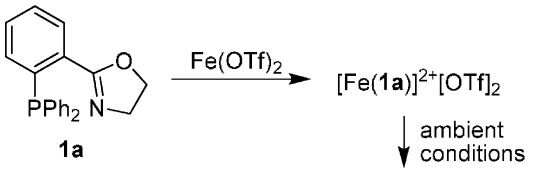

(1)

The coordination of two PHOX ligands to the iron center in **3a** and **b** could clearly be established by IR and MS. The free ligands **1a** and **b** give characteristic $\nu_{C=N}$ stretching frequencies of 1644 and 1630 cm^{-1}, which shift significantly to lower wavenumbers (1627 and 1604 cm^{-1}), when coordinated to the iron center. This phenomenon is exemplified for complex **3a** in Fig. 2, which shows traces of the free ligand **1a** (top trace) and the neat complex **3a** (middle trace). The IR spectra also provide evidence for the position of the OTf counterion in the solid state. Free OTf counterions give IR absorptions at 1268, 1223, 1143, and 1030 cm^{-1}, assigned to S–O and C–F stretches [12]. As analyzed by van Koten and Klein Gebbink [13], coordination of one oxygen atom to an iron center desymmetrizes the OTf ion, leading to multiple S–O absorptions,

Table 1
Screening of catalyst activity

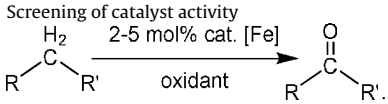

Entry	Substrate	Oxidant[a]	Time/temperature	Catalyst[b]	Product	Conversion (%)[c]	TOF[d] (h^{-1})
1	Cinnamyl alcohol	Me_3NO	44 h/rt	**2c**	Cinnamyl aldehyde	39	0.18
2	Diphenylmethane	*t*-BuOOH	18 h/90 °C	**2c**	Benzophenone	71	0.79
3	Dihydroanthracene	*t*-BuOOH	9 h/90 °C	**2c**	Anthraquinone	56	1.24
4	Fluorene	*t*-BuOOH	18 h/90 °C	**2c**	Fluorenone	5	0.06
5	Cyclohexane	Me_3NO or H_2O_2	72 h/rt	**3a**	NR		
6	Toluene	H_2O_2	30 h/rt	**3a**	NR		
7	Toluene	*t*-BuOOH	30 h/rt	**3a**	Benzaldehyde	Traces	–
8	Cyclooctadiene	*t*-BuOOH	24 h/80 °C	**3a**	NR		
9	*p*-Cymene	H_2O_2	32 h/80 °C	**3a**	NR		
10	Dimethoxytoluene	*t*-BuOOH	20 h/80 °C	**3a**	NR		
11	Cinnamyl alcohol	*t*-BuOOH	24 h/80 °C	**3a**	NR		
12	Tetrahydronaphthalene	*t*-BuOOH	22 h/80 °C	**3a**	NR		
13	Fluorene	*t*-BuOOH	22 h/rt	**3a**	Fluorenone	100	2.3
14[e]	Fluorene	*t*-BuOOH plus TEMPO	18 h/rt	**3a**	Fluorenone	51	0.56
15	Diphenylmethane	*t*-BuOOH	22 h/rt	**3a**	Benzophenone	64	1.45
16	Diphenylmethane	*t*-BuOOH	18 h/rt	$Fe(\mathbf{1a})_2Cl_2$	Benzophenone	38	0.86
17	Fluorene	*t*-BuOOH	22 h/rt	$Fe(\mathbf{1a})_2Cl_2$	Fluorenone	84	1.90
18	Fluorene	*t*-BuOOH	22 h/rt	$Fe(OTf)_2$	Fluorenone	77	1.75

[a] Oxidants were used in 2–3.5-fold excess.
[b] 5 mol% **2c**, 2 mol% **3a**, $Fe(\mathbf{1a})Cl_2$ and $Fe(OTf)_2$.
[c] Determined by GC/MS.
[d] Number of moles (product) over number of moles (catalyst) times the reaction time. Derived from GC data.
[e] Identical conditions to entry 13, but in presence of 20 mol% TEMPO.

one being shifted to 1310 cm^{-1}. We did not observe such a strong effect in the iron complex **3a**. However, as shown in Fig. 2 (middle trace, neat complex), the band at 1259 cm^{-1} exhibits shoulders, which might be attributed to a weak coordination of the OTf ion to the iron center, which is clearly advantageous for potential catalytic applications. This weak interaction is further corroborated by an IR spectrum recorded in the coordinating solvent acetonitrile (Fig. 2, bottom trace). Acetonitrile coordinates to the metal center, as shown by a new absorption at 2293 cm^{-1} (not shown); the S–O absorption is shifted to 1265 cm^{-1} and shows no shoulders, as would be expected for a non-coordinated OTf ion.

The FAB MS spectra of **3a** and **b** also confirm the general formulation $[Fe(\mathbf{1a})_2]^{2+}[OTf]_2$ and $[Fe(\mathbf{1b})_2]^{2+}[OTf]_2$ for the two complexes. Complex **3a** exhibits a molecular ion peak corresponding to the formula $[Fe(\mathbf{1a})_2(OTf)]^+$ and a fragment of the formula $[Fe(\mathbf{1a})(OTf)]^+$. A peak for $[Fe(\mathbf{1a})(OTf)(H_2O)]^+$ was also detected. The open coordination site in this formulation is occupied with water; no OH frequencies were observed in the solid-state material by IR, and the water molecules probably originate from the FAB matrix. For complex **3b**, only a molecular ion corresponding to $[Fe(\mathbf{1b})_2(O)(Tf)]^+$ could be observed. Based on the spectroscopic data available for the complexes, it cannot be determined what the position of the oxygen in the molecule is and from where it originates. We assume that the complex absorbs water from the FAB matrix or the atmosphere, and the corresponding deprotonated species is detected in the MS data. The elemental analysis for **3b** is low in carbon, also suggesting that extra water molecules may be present in the material, consistent with the observed hygroscopic nature of solid **3b**.

The iron complexes **3a** and **b** are paramagnetic. For **3a**, a magnetic moment of μ_{eff} = 2.26 BM was determined by the Evans method [9]. This value is lower than that expected from the spin-only formula (4.9 BM) for an octahedral Fe(II) complex with high spin configuration (S = 2). Either the complex does not have an ideal octahedral configuration or spin-crossover may be taking place, which is not uncommon for octahedral iron complexes with nitrogen donor ligands [14]. For **3b**, a higher magnetic moment of μ_{eff} = 3.63 BM was determined. Consequently, the novel iron complexes gave very poor NMR spectra. For complex **3b**, only very broad ^1H and ^{13}C NMR resonances were observed, and no signals at all were detected in the ^{31}P NMR spectra of any of the new complexes. However, complex **3a** gave reasonable ^1H and ^{13}C NMR spectra with some line broadening (spectra see Supporting Material). For the eight diastereotopic CH_2 protons of the two oxazoline rings in the complex, six broad signals were observed in the proton NMR spectrum. In the ^{13}C NMR, the aromatic region of the spectrum is not very well resolved. However, for the carbon atoms of oxazoline rings, a double set of signals were observed in the ^{13}C NMR, establishing that the two oxazoline rings in the complex are not equivalent.

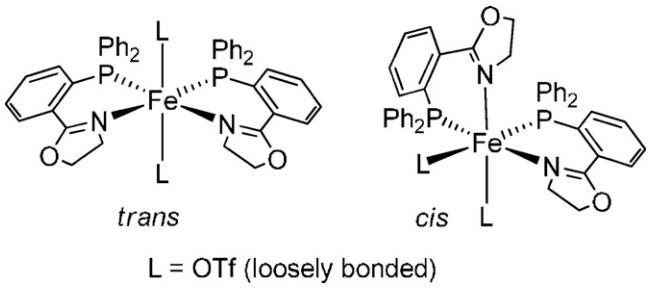

Fig. 3. Potential cis and trans isomers for complex **3a**.

All attempts to obtain X-ray quality crystals of one of the complexes have failed thus far. As the complexes **3a** and **b** cannot be analyzed by ^{31}P NMR, a definitive structure for the two complexes could not be established. However, a close examination of the IR spectrum of **3a** (Fig. 2, middle trace) revealed two $\nu_{C=N}$ stretching frequencies, suggesting two non-equivalent nitrogen donor atoms in the coordination spheres of the complex. The available NMR spectra for this complex suggest two non-equivalent oxazoline rings. This data is well in accordance with a cis isomer (Fig. 3) for complex **3a**. In the cis isomer, the two oxazoline rings are non-equivalent, as well as the two nitrogens, as each has a different ligand in the trans position. Complex **3b** exhibited only one $\nu_{C=N}$ stretching frequency in the IR, but as opposed to **3a**, it did not give an elemental analysis in the acceptable range and much poorer NMR spectra. Thus, our further investigations focused on the complex **3a**.

3.2. Catalytic oxidation reactions

We next employed the complexes **2c** (Fig. 1) and **3a** as catalysts for initial screening of different hydrocarbon substrates and oxidants, and the results are compiled in Table 1. The screening experiments revealed that both complexes are catalytically active in the oxidation of activated (benzylic) methylene groups to give ketones. Cyclohexane, cyclooctene, the methine group in triphenylmethane, as well as adamantane could not be oxidized under the reaction conditions employed herein, and gave at most trace quantities of the products. Hydrogen peroxide H_2O_2 could not be employed, but *t*-BuOOH was generally suitable as oxidant, and a two- to threefold excess over the substrate gave the best results. Ketones were typically the only reaction products; alcohols were

Table 2
Iron catalyzed oxidation reactions

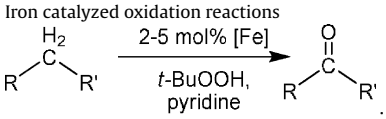

Entry	Substrate	Product	Catalyst	Yield[a]	TOF (h^{-1})[b]
1[c]	Diphenylmethane	Benzophenone	**2c**	68%	0.76
2[c]	Dihydroanthracene	Anthraquinone	**2c**	49%	1.1
3[d]	Fluorene	Fluorenone	**3a**	91%	3.8
4[e]	Fluorene	Fluorenone	**3a**	93%	3.9
5[d]	Dihydroanthracene	Anthraquinone	**3a**	38%	1.4
6[d]	Diphenylmethane	Benzophenone	**3a**	43%	1.6
7[f]	Fluorene	Fluorenone	$Fe(OTf)_2$	80%	1.7

[a] Isolated yields after column chromatography or extraction.
[b] Determined from isolated yield: number of moles (product) over number of moles (catalyst) times reaction time.
[c] Conditions: substrate (0.30 mmol), catalyst **2c** (5 mol%), *t*-BuOOH (3.5 equiv.), 18 h (9 h for dihydroanthracene) in pyridine (1 mL) at 90 °C.
[d] Conditions: substrate (0.60 mmol), catalyst **3a** (2 mol%), *t*-BuOOH (1.8–2 equiv.), 12 h in pyridine (2 mL) at room temperature.
[e] Conditions identical to those in [b] but under an atmosphere of argon.
[f] Conditions: substrate (0.30 mmol), catalyst $Fe(OTf)_2$ (2.8 mol%), *t*-BuOOH (2 equiv.), 18 h in pyridine (1 mL) at room temperature.

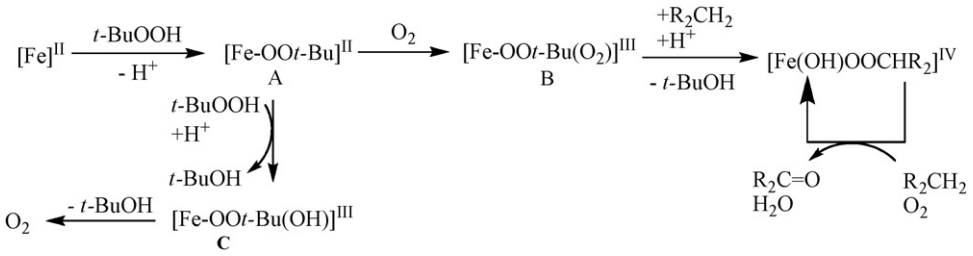

Scheme 2. Simplified mechanism for "oxygenated Fenton chemistry" proposed by Sawyer [15b].

not observed by GC/MS. Complex **2c** (5 mol%) required elevated reaction temperatures of 90 °C for catalytic activity, whereas **3a** (2 mol%) could be employed at room temperature under optimized conditions (entry 13). Pyridine was determined to be the solvent of choice. The precursor complex $Fe(OTf)_2$ also showed activity in the oxidation of fluorene (*vide infra*). Without catalysts, at most, trace quantities of products were observed in the reaction mixtures.

Under optimized reaction conditions, complexes **2c** and **3a** were then utilized in the oxidation of a variety of substrates, as compiled in Table 2. Diphenylmethane, fluorene and anthracene were oxidized to the corresponding ketones in 93–38% isolated yields after column chromatography. About a twofold excess of *t*-BuOOH with a catalyst loading of 5 mol% in pyridine as solvent was employed. Turnover frequencies ranging from 0.76 to 4.2 h^{-1} were determined. The iron salt $Fe(OTf)_2$ also catalyzed the oxidation of fluorene to fluorenone under the conditions applied for **3a** (Table 2, entry 7). Bolm showed that $FeCl_3$ catalyzes benzylic oxidations with aqueous *t*-BuOOH [2i] and Britovsek showed that $Fe(OTf)_2$ oxidizes cyclohexane with H_2O_2 to give an alcohol/ketone mixture [2j]. As mentioned above, the coordinatively saturated iron complex **2c** required reaction temperatures of 90 °C and produced lower turnover frequencies than **3a**. We hypothesized that complex **2c** first needs to generate an open coordination site by thermal ligand loss, whereas **3a** has two coordination sites, which are only loosely occupied by OTf counterions (Fig. 1). As already established in the preliminary screening experiments (Table 1), non-activated alkanes and allylic methylene groups were not oxidized under the reaction conditions described herein.

3.3. Further experiments to understand the mechanism of the title reaction

Iron–hydroperoxide induced oxidation of alkanes is a field of intensive study [15]. The mechanism and participating intermediates strongly depend on the reaction conditions, solvents, oxidants and the relative ratio of the substrates [16]. In the present catalytic experiments, alcohols were not observed as oxidation products and we only isolated the corresponding ketones. This product profile is in accordance with a mechanism described by Sawyer as "oxygenated Fenton chemistry" (Scheme 2 shows a simplified mechanism) [15b]. The Fe(II) first forms an alkylperoxo species **A**, which takes up oxygen to form **B**; compound **B** converts methylene groups to ketones, and can be regenerated by reaction with R_2CH_2 and oxygen. The oxygen needed for the reaction could be provided by the atmosphere, but Fe(II) complexes are also known to disproportionate peroxides to give oxygen. Thus, the oxygen for the catalytic reaction might also be provided by *t*-BuOOH decomposition, and accordingly we also observed catalytic activity under an argon atmosphere (Table 2, entry 4).

To investigate whether or not species **A** plays a role in our catalytic systems, UV–vis spectra of the iron catalyst **3a** were recorded, and the traces are shown in Fig. 4. Complex **3a** exhibits a broad band around 350 nm and a peak at 247 nm (black trace). However, upon addition of *t*-BuOOH, immediately a new broad band around 420 nm appeared in the UV–vis spectrum (Fig. 4, grey trace). After 24 h, this band is replaced (or hidden) by a much stronger absorption centered around 280 nm (spectrum see Supplementary Material). Due to the appearance of this strong band, formation or decay of the new UV–vis band at 420 nm could not be followed over time, as performed by other researchers.

The band around 420 nm might indeed be due to the formation of the peroxo species **A** (Scheme 2). Several authors described this species to be formed from iron complexes and *t*-BuOOH, and to give a LMCT band between 500 and 600 nm in the UV–vis spectra [15 g, 17]. These values are at least in the order of the new absorption observed in our spectra after addition of *t*-BuOOH.

Alkylperoxo species such as **A** are known to undergo either homolytic or heterolytic O–O bond cleavage to give high valent iron oxo species [Fe=O], which are also reported to be potential intermediates in iron catalyzed oxidation reactions [18]. However, this species is reported to be involved in the formation of alcohols from alkanes and epoxides from alkenes [19], which were never observed in our experiments. Furthermore, iron oxo species [Fe=O] are reported to give UV–vis absorptions around 750 nm [20] and no absorptions above 600 nm were observed.

The question as to whether or not a radical species is involved in our reaction could on the other hand also not be definitely excluded. The reaction slows slightly when run in the presence of 20 mol% TEMPO (2,2,6,6-tetramethylpiperidine-1-oxyl, a scavenger for carbon-centered radicals), but it did not completely stop (entry 14, Table 1). The title reaction is often run with a large excess of the substrate in order to avoid overoxidation of alcohol products to ketones. When we run our reaction with a 500:50:10 ratio of fluorene:*t*-BuOOH:**3a** (Scheme 3), we observed the dihydrofluorene species **4** and the fluorene dimer **5** in the reaction mixture by GC/MS. These compounds might be derived from radicals under these reaction conditions, but besides the ketone product (fluorenone) no alcohol was observed in the reaction mixture. A reaction under standard conditions in Table 2 with adamantane gave little reaction products; but trace quantities of alcohol, ketone and pyridyl substituted adamantyl products were detected, also sug-

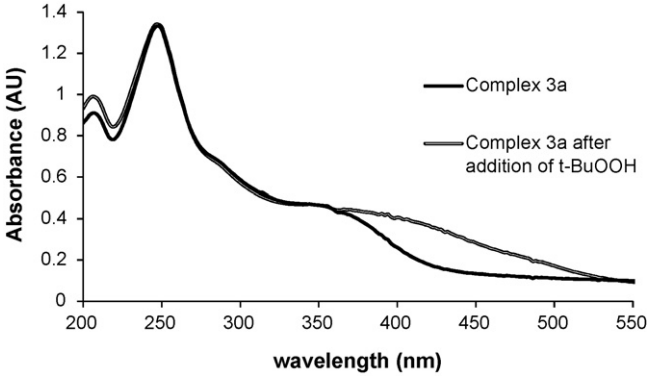

Fig. 4. UV–vis spectra of complex **3a** before and after addition of *t*-BuOOH.

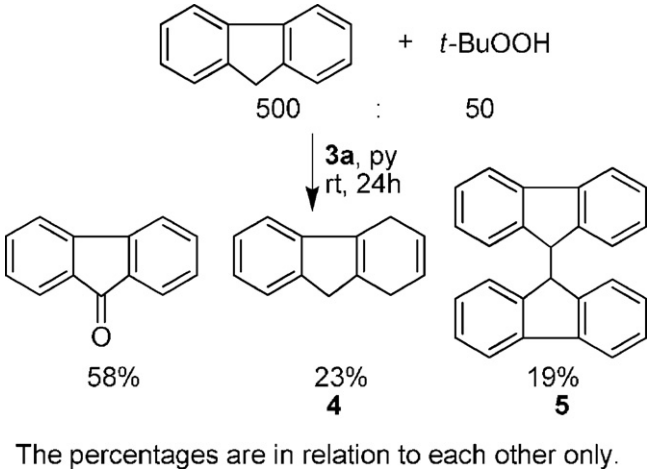

Scheme 3. GC/MS experiment to investigate a potential radical mechanism.

gesting the participation of radical species. These findings clearly give some evidence for radical involvement in the reactions, but the lack of alcohol products in our reactions in Table 2 might be better explained by the mechanism shown in Scheme 2.

Finally, we followed the substrate consumption for the reaction of fluorene (entry 3 in Table 2) over 5 h at room temperature by GC/MS employing the catalysts **3a**, $[Fe(\mathbf{1a})(H_2O)_n]^{2+}[OTf]_2$ and $Fe(OTf)_2$. The result for the complex **3a** is shown in Fig. 5. The other two complexes showed a similar profile, and the traces are given in the Supporting Material. The catalyzed reactions appeared to follow a pseudo zero order rate law in substrate, which has previously been reported for other catalyzed reactions [21]. The observed rate constants were determined from the slope of the line in Fig. 5 to be 0.059 min^{-1} for **3a**, 0.064 min^{-1} for $[Fe(\mathbf{1a})(H_2O)_n]^{2+}[OTf]_2$ and 0.092 min^{-1} for $Fe(OTf)_2$ (see Supporting Material). Fig. 6 compiles the linear trends for the catalytic experiments in one graph. The data reveal that the complex $[Fe(\mathbf{1a})(H_2O)_n]^{2+}[OTf]_2$ with one PHOX ligand in its coordination sphere is about comparable to catalyst **3a**. In turn, the rate constant of $Fe(OTf)_2$ is somewhat higher than that of

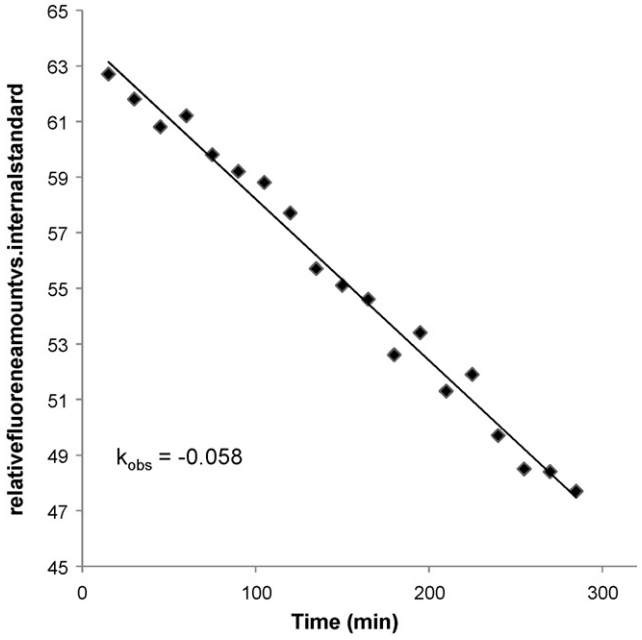

Fig. 5. Decay of fluorene for the reaction in entry 3 (Table 2) over time employing **3a** as catalyst.

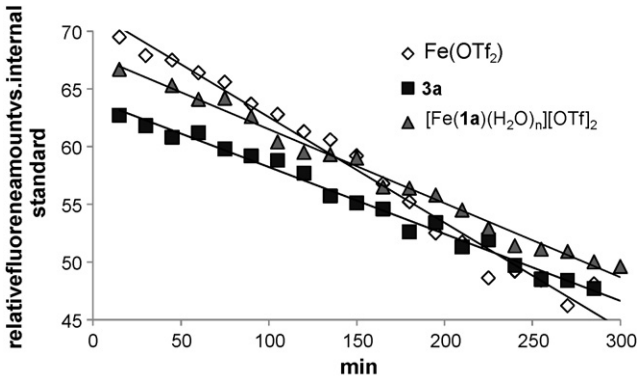

Fig. 6. Decay of fluorene for the reaction in entry 3 (Table 2) over time for different catalysts.

complex **3a**. The increased rate constant of $Fe(OTf)_2$ might again be ascribed to the need for open coordination sites on the iron center for catalytic activity.

As of now, we do not have conclusive data what the catalytically active species in the catalytic cycle might be. The kinetic data in Fig. 6 suggest that **3a** and $[Fe(\mathbf{1a})(H_2O)_n]^{2+}[OTf]_2$ form identical catalytically active species in solution. To obtain information about its identity, complex **3a** was subjected to conditions identical to those in Table 2, but in the absence of any substrate. The resulting residue was analyzed by IR and MS. New IR stretching frequencies were observed at 1666, 1611 and 1600 cm^{-1}, which are different from **3a** and the free PHOX ligand **1a**. In the MS, only a peak corresponding to the formulation $[Fe(\mathbf{1a})(O)_2(pyridine)(OTf)]^+$ could unambiguously assigned. However, it seems unlikely that **3a** first looses both PHOX ligands to form a catalytically active species identical to the one formed by $Fe(OTf)_2$ alone. The rate constants for **3a** and $Fe(OTf)_2$ are different. Furthermore, no induction period was observed in the kinetic investigations for **3a** and $[Fe(\mathbf{1a})(H_2O)_n]^{2+}[OTf]_2$ (Figs. 5 and 6), which makes it unlikely that both species first lose their chelating PHOX ligands prior to developing catalytic activity.

4. Conclusion

The present study shows for the first time the catalytic activity of iron PHOX complexes of the general formula $[Fe(PHOX)_2]^{2+}$ in the oxidation of activated methylene groups to ketones with an excess of *t*-BuOOH as the oxidant. The isolated yields ranged from 38 to 93%, no alcohols were detected during the course of the reaction, and the catalyst load was 2 mol%. The catalyst design allows the reaction to proceed at room temperature, as opposed to the previously synthesized iron complexes of the general formula $[Fe(Cp)(CO)(PHOX)]^+[I]^-$, which only show catalytic activity at 90 °C. The lack of alcohols as the reaction products is in accordance with "oxygenated Fenton chemistry" previously described by other authors. UV–vis spectra of the reaction between one of our iron complexes and an excess of *t*-BuOOH suggested an intermediate alkylperoxo species $[Fe–OO\mathit{t}–Bu]^{II}$ which are also reported in the "oxygenated Fenton chemistry". Kinetic experiments revealed that the reaction is pseudo zero order in the substrate, and that the mono-coordinated iron PHOX complex $[Fe(PHOX)]^{2+}$ performs comparable to the di-coordinated complex $[Fe(PHOX)_2]^{2+}$.

Acknowledgements

We thank Dr. Wesley Harris (University of Missouri – St. Louis) for assistance with the UV–vis spectra and Alemu Azanaw for technical assistance in performing the kinetic studies. We thank the

University of Missouri – St. Louis for support. Funding from the National Science Foundation for the purchase of the NMR spectrometer (CHE-9974801) and the purchase of the mass spectrometer (CHE-9708640) are acknowledged.

Appendix A. Supplementary data

Supplementary data associated with this article can be found, in the online version, at doi:10.1016/j.molcata.2009.05.002.

References

[1] (a) E.B. Bauer, Curr. Org. Chem. 12 (2008) 1341;
(b) A. Correra, O. Garcia Mancheño, C. Bolm, Chem. Soc. Rev. 37 (2008) 1108;
(c) B.D. Sherry, A. Fürstner, Acc. Chem. Res. 41 (2008) 1500;
(d) C. Bolm, J. Legros, J. Le Paih, L. Zani, Chem. Rev. 104 (2004) 6217;
(e) M. Costas, M.P. Mehn, M.P. Jensen, L. Que Jr., Chem. Rev. 104 (2004) 939;
(f) E.Y. Tshuva, S.J. Lippard, Chem. Rev. 104 (2004) 987.
[2] Most recent examples of iron catalysis:
(a) W.M. Czaplik, M. Mayer, A. Jacobi von Wangelin, Angew. Chem. Int. Ed. 48 (2009) 607;
(b) M. Nakanishi, A.-F. Salit, C. Bolm, Adv. Synth. Catal. 350 (2008) 1835;
(c) Y. Feng, C. Ke, G. Xue, L. Que Jr., Chem. Commun. (2009) 50;
(d) M.S. Chen, M.C. White, Science 318 (2007) 783;
(e) C.P. Casey, H. Guan, J. Am. Chem. Soc. 131 (2009) 2499;
(f) C. Wallenhorst, G. Kehr, H. Luftmann, R. Fröhlich, G. Erker, Organometallics 27 (2008) 6547;
(g) S. McTavish, G.J.P. Britovsek, T.M. Smit, V.C. Gibson, A.J.P. White, D.J. Williams, J. Mol. Catal. A: Chem. 261 (2007) 293;
(h) S. Prateeptongkum, I. Jovel, R. Jackstell, N. Vogl, C. Weckbecker, M. Beller, Chem. Commun. (2009) 1990;
(i) M. Nakanishi, C. Bolm, Adv. Synth. Catal. 349 (2007) 861;
(j) G.J.P. Britovsek, J. England, S.K. Spitzmesser, A.J.P. White, D.J. Williams, Dalton Trans. (2005) 945.
[3] (a) D.P. Barbosa Souza, A.T. Fricks, H.M. Alvarez, G.C. Salomao, M.H. Neves Olsen, L. Cardozo Filho, C. Fernandes, O.A.C. Antunes, Catal. Commun. 8 (2007) 1041;
(b) A. Fürstner, E. Kattnig, O. Lepage, J. Am. Chem. Soc. 128 (2006) 9194.
[4] S.L. Sedinkin, N.P. Rath, E.B. Bauer, J. Organomet. Chem. 693 (2008) 3081.
[5] (a) P. von Matt, A. Pfaltz, Chem. Angew, Int. Ed. Engl. 32 (1993) 566;
(b) J. Sprinz, G. Helmchen, Tetrahedron Lett. 34 (1993) 1769;
(c) G.J. Dawson, C.G. Frost, J.M. Williams, S.J. Coote, Tetrahedron Lett. 34 (1993) 3149.
[6] (a) G. Helmchen, A. Pfaltz, Acc. Chem. Res. 33 (2000) 336;
(b) H.A. McManus, P.J. Guiry, Chem. Rev. 104 (2004) 4151.
[7] P. Braunstein, G. Clerc, X. Morise, New J. Chem. 27 (2003) 68.
[8] K.S. Hagen, Inorg. Chem. 39 (2000) 5867.
[9] (a) D.F. Evans, J. Chem. Soc. (1959) 2003;
(b) G.S. Girolami, T.B. Rauchfuss, R.J. Angelici, Synthesis and Technique in Inorganic Chemistry, third ed., University Science Books, Mill Valley, 1999.
[10] The most intense peak of isotope envelope (relative intensity, %) is listed.
[11] The complex Fe(**1a**)$_2$Cl$_2$ was synthesized under conditions identical to those for the synthesis of [Fe(**1a**)$_2$][OTf]$_2$. The isolated complex was characterized by IR and MS, and both spectra are given in the Supplementary Material. One strong C=N band at 1627 cm^{-1} was observed for the coordinated PHOX ligand **1a** and no band for the uncoordinated ligand was detected. The MS spectrum exhibited peaks for molecules of the formula [Fe(**1a**)$_2$Cl]$^+$ and [Fe(**1a**)$_2$Cl(O)]$^+$. However, the spectrum exhibited also a peak according to the formula [Fe(**1a**)Cl]$^+$. This peak might either be due to a fragment or a complex of the formula Fe(**1a**)$_1$Cl$_2$ containing only one PHOX ligand may also be present in the isolated material.
[12] M. Aresta, A. Dibenedetto, E. Amodio, I. Pápai, G. Schubert, Inorg. Chem. 41 (2002) 6550.
[13] S. Gosiewska, J.J.L.M. Cornelissen, M. Lutz, A.L. Spek, G. van Koten, R.J.M. Klein Gebbink, Inorg. Chem. 45 (2006) 4214.
[14] (a) A. Bousseksou, G. Molnár, J.A. Real, K. Tanaka, Coord. Chem. Rev. 251 (2007) 1822;
(b) M. Arai, W. Kosaka, T. Matsuda, S. Ohkoshi, Angew. Chem. Int. Ed. 47 (2008) 688;
(c) B. Weber, W. Bauer, J. Obel, Angew. Chem. Int. Ed. 47 (2008) 10098.
[15] (a) H. Sugimoto, D.T. Sawyer, J. Am. Chem. Soc. 107 (1985) 5712;
(b) D.T. Sawyer, A. Sobkowiak, T. Matsushita, Acc. Chem. Res. 29 (1996) 409;
(c) C. Walling, Acc. Chem. Res. 31 (1998) 155;
(d) P.A. MacFaul, D.D.M. Wayner, K.U. Ingold, Acc. Chem. Res. 31 (1998) 159;
(e) D.H.R. Barton, D. Doller, Pure Appl. Chem. 63 (1991) 1567;
(f) A. Rabion, R.M. Buchanan, J.-L. Seris, R.H. Fish, J. Mol. Catal. A: Chem. 116 (1997) 43;
(g) F.G. Gelalcha, G. Anilkumar, M.K. Tse, A. Brückner, M. Beller, Chem. Eur. J. 14 (2008) 7687.
[16] F. Gozzo, J. Mol. Catal. A: Chem. 171 (2001) 1.
[17] (a) F. Namuswe, G.D. Kasper, A.A. Narducci Sarjeant, T. Hayashi, C.M. Krest, M.T. Green, P. Moënne-Loccoz, D.P. Goldberg, J. Am. Chem. Soc. 130 (2008) 14189;
(b) M.P. Jensen, A. Mairata i Payeras, A.T. Fiedler, M. Costas, J. Kaizer, A. Stubna, E. Münck, L. Que Jr., Inorg. Chem. 46 (2007) 2398;
(c) M.R. Bukowski, H.L. Halfen, T.A. van den Berg, J.A. Halfen, L. Que Jr., Angew. Chem. Int. Ed. 44 (2005) 584;
(d) M.P. Jensen, M. Costas, R.Y.N. Ho, J. Kaizer, A. Mairata i Payeras, E. Münck, L. Que Jr., J.-U. Rohde, A. Stubna, J. Am. Chem. Soc. 127 (2005) 10512;
(e) M.P. Jensen, S.J. Lange, M.P. Mehn, E.L. Que, L. Que Jr., J. Am. Chem. Soc. 125 (2003) 2113.
[18] (a) N.A. Stephenson, A.T. Bell, Inorg. Chem. 46 (2007) 2278;
(b) M. Sook Seo, T. Kamachi, T. Kouno, K. Murata, M. Joo Park, K. Yoshizawa, W. Nam, Angew. Chem. Int. Ed. 46 (2007) 2291.
[19] A. Agarwala, D. Bandyopadhyay, Catal. Lett. 124 (2008) 256.
[20] Y. Zhou, X. Shan, R. Mas-Ballesté, M.R. Bukowski, A. Stubna, M. Chakrabarti, L. Slominski, J.A. Halfen, E. Münck, L. Que Jr., Angew. Chem. Int. Ed. 47 (2008) 1896.
[21] R.V. Chaudhari, A. Seayad, S. Jayasree, Catal. Today 66 (2001) 371.